International Journal of Engineering Research and Development
e-ISSN: 2278-067X, p-ISSN: 2278-800X, www.ijerd.com
Volume 11, Issue 12 (December 2015), PP.01-12

Co-ordinated control of FACTS Devices using Optimal Power Flow Technique

S. Raghavendra Rao[1], Ch. Padmanabha Raju[2]
[1]*PG Scholar, Department of Electrical & Electronics Engineering, P.V.P. Siddhartha Institute of Technology, Vijayawada, A.P-520007*
[2]*Professor, Department of Electrical & Electronics Engineering, P.V.P. Siddhartha Institute of Technology Vijayawada, A.P -520007*

Abstract:-The Optimal Power Flow (OPF) plays an important role in power system operation and control due to depleting energy resources, and increasing power generation cost and ever growing demand for electrical energy. Here FACTS devices are effectively used for power flow control, voltage regulation, improvement of power system stability, minimization of losses. The FACTS devices that we use are SVC and UPFC. For power flow studies, the modeling of FACTS devices is discussed. The SVC is good at voltage regulation and UPFC is good at balancing the reactive power in the system. In this paper, PSO based approach is presented to solve the Optimal Power Flow to satisfy objectives such as minimizing generation cost and transmission line loss. The proposed PSO algorithm is tested on IEEE 30 bus system.

Keywords:- Mathematical model of OPF, SVC, UPFC, Co-ordinate control, PSO, Cost of generation.

I. INTRODUCTION

The rapid growth of heavy loads in the system and high power transfer on the line makes it uncomfortable. Due to this the line may get damage and construction of additional lines or siting new generation is very difficult. For avoiding these problem FACTS devices is introduced. FACTS technology makes power system easy to transfer the active power without overloading the line. FACTS devices can be effectively used for power flow control, voltage regulation, improvement of power system stability, minimization of losses. In the power system cost is also the main thing that we need take into the consideration .In order to investigate the effects of FACTS devices in steady-state, appropriate models are needed capturing the influences of the devices on power flows and voltages. Various models for SVC, and UPFC are conceivable and applied in different studies. In Sect. II, the modelling of FACTS devices that we used in this paper and how they are incorporated into the power flow calculations are described.

A static VAR compensator is a set of electrical devices for providing fast-acting reactive power on high-voltage electricity transmission networks. SVCs are part of the Flexible AC transmission system device family, regulating voltage, power factor, and harmonics and stabilizing the system. Unlike a synchronous condenser which is a rotating electrical machine, a static VAR compensator has no significant moving parts (other than internal switchgear). Prior to the invention of the SVC [1], power factor compensation was the preserve of large rotating machines such as synchronous condensers or switched capacitor banks.

A combination of static synchronous compensator (STATCOM) and a static synchronous series compensator (SSSC) which are coupled via a common dc link, to allow bidirectional flow of real power between the series output terminals of the SSSC and the shunt output terminals of the STATCOM, and are controlled to provide concurrent real and reactive series line compensation without an external electric energy source. The UPFC, by means of angularly unconstrained series voltage injection, is able to control, concurrently or selectively, the transmission line voltage, impedance, and angle or, alternatively, the real and reactive power flow in the line. The UPFC may also provide independently controllable shunt reactive compensation. In section III it shows about the mathematical formulation of the optimal power flow of the system.

In sec IV the influences of FACTS devices are not confined to one bus or line. Changing the voltage at a certain bus or the power flow on a line also modifies the power flow in the surrounding grid. If a FACTS device is placed in the vicinity of another, mutual influences may arise which could vitiate the positive impacts of a single device. So by using this Co-ordinate control on the FACTS devices we can reduce the influence of one device on another. Therefore the sec V invesgates about the different cases there first we consider the normal case means without introducing FACTS devices and in the next case by introducing single and multiple FACTS devices we calculate cost of generation, power losses, sum of squares of voltage stability indices and CPU time in each case.

II. MATHEMATICAL MODEL OF FACTS DEVICES

2.1 Modelling of SVC:

According to IEEE the definition of the SVC [1],[2] is as follows "A shunt connected static var generator or absorber whose output is adjusted to exchange capacitive or inductive current so as to maintain or control specific parameters (typically bus voltage) of the electrical power system.

SVC device is a parallel combination of thyristor controlled reactor with a bank of capacitors. It's a shunt connected variable reactance, which either generates or absorbs reactive power in order to regulate the voltage magnitude where it is connected to the AC network. Mainly used for voltage regulation. As an important component for voltage control, it is usually installed at the receiving node of the transmission lines.

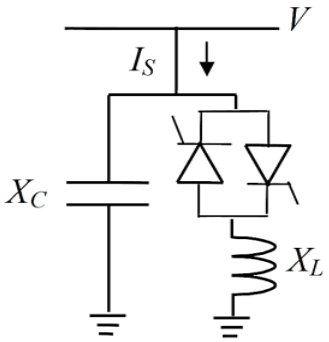

Fig 1 FC-TCR structure of SVC.

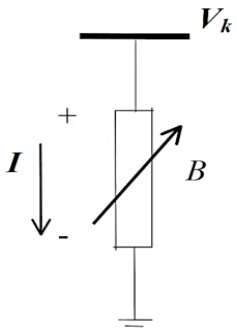

Fig 2 Variable-Shunt Susceptance.

With reference to the above figure, the current drawn by the SVC is

$$I_{svc} = jB_{svc}V_k \quad (1)$$

and the reactive power drawn by the SVC, which is also the reactive power injected at bus k, is

$$Q_{svc} = Q_k = -V_k^2 B_{svc} \quad (2)$$

where the equivalent Susceptance B_{svc} is taken to be the state variable

$$\begin{bmatrix}\Delta P_k \\ \Delta Q_k\end{bmatrix}^{(i)} = \begin{bmatrix}0 & 0 \\ 0 & Q_k\end{bmatrix}^{(i)} \begin{bmatrix}\Delta\theta_k \\ \Delta B_{svc}/B_{svc}\end{bmatrix}^{(i)} \quad (3)$$

At the end of iteration (i), the variable shunt susceptance B_{svc} is updated according to

$$B_{svc}^{(i)} = B_{svc}^{(i-1)} + \left(\frac{\Delta B_{svc}}{B_{svc}}\right)^{(i)} B_{svc}^{(i)} \quad (4)$$

The changing susceptance represents the total SVC susceptance necessary to maintain the nodal voltage magnitude at the specified value. Once the level of compensation has been computed then the thyristor firing angle can be calculated. However, the additional calculation requires an iterative solution because the SVC susceptance and thyristor firing angle are nonlinearly related.

2.2 SVC in the transmission network:

The SVC based on thyristor without the gate turn-off capability is considered as a shunt connected static Var generator or absorber, whose output is adjusted to exchange capacitive or inductive current. It is an important component for voltage control in power systems and is usually installed at the receiving bus bar. In the power flow formulation, the SVC has been considered as a reactive power source within the reactive power limits set by available inductive and capacitive susceptanc

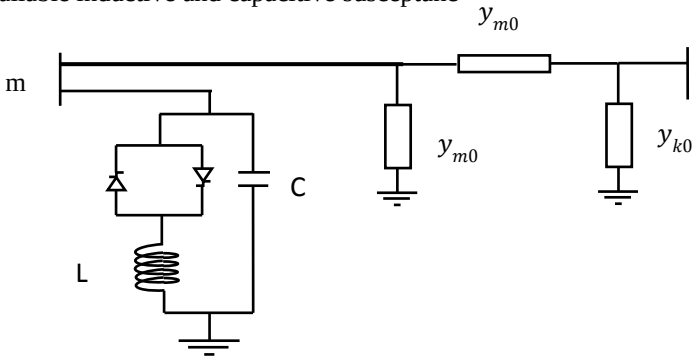

Fig 3 SVC inserting in a line

SVC placed at the beginning of the line

For an SVC connected at a bus bar m of a line section represented by the quadruple (y_{mo} ,y_{mk} , y_{ko}) as shown in figure, the contribution of the SVC to the new admittance matrix relates to the element shunt. It results in the admittance matrix of the line.

$$Y_{new}^{line} = \begin{bmatrix} y_{mk} + y_{mo} + y_{svc} & -y_{mk} \\ -y_{mk} & y_{mk} + y_{ko} \end{bmatrix} \quad (5)$$

We know such that

$$B_{svc} = \frac{1}{X_{svc}}$$

$$B_{svc} = \frac{1}{X_C X_L}\left\{X_L - \frac{X_C}{\pi}[2(\pi - \alpha) + \sin 2\alpha]\right\} \quad (6)$$

The SVC reactance is given as following

$$X_{svc}(\alpha) = \frac{\pi X_L}{2(\pi-\alpha)+\sin(2\alpha)-\pi\frac{X_L}{X_C}} \quad (7)$$

Influence of the SVC on the network

It results from these modifications on the nodal admittances matrix and from the Jacobian. These modifications are detailed in what follows.

Modification of the admittances matrix*:*

We modelled the SVC as being a variable transverse admittance which is connected to a bus m of the network. Thus, the effect of this is based only on the modification of the element y in the admittances matrix. The new modified matrix is written as follows:

$$Y_{new} = \begin{bmatrix} Y_{11} \cdots & Y_{1m} & \cdots Y_{1n} \\ \vdots \ \ddots & \vdots & \iddots \ \vdots \\ Y_{m1} \cdots Y_{mm}^{old} & + Y_{svc} & \cdots Y_{mn} \\ \vdots \ \iddots & \vdots & \ddots \ \vdots \\ Y_{n1} \cdots & Y_{nm} & \cdots Y_{nn} \end{bmatrix} \quad (8)$$

This new matrix is used to calculate the new power transit. By varying the firing angle of the SVC "α", it is possible to plot the curves of voltages variation at the buses. They allow locating the best point of compensation of the network. The variation curves of the powers losses in the lines can be obtained according to "α" which makes it possible to measure the impact of the SVC device on these lines. These curves will be studied for the compensation of a network in the overvoltage.

The impact of the nature of the load and its importance will be observed by studying two loading cases purely active and reactivate respectively. While varying the load at the bus to which the SVC is connected and by maintaining "α" constant, the curves of voltages variation as well as those of the power losses will be plotted.

Modification of the Jacobian matrix:

To take into account the introduction of the SVC as a voltage regulator and thus to allow the program to calculate the ideal firing angle to maintain the bus voltage where it is inserted to a consign value, it is necessary to introduce modifications into the Jacobian matrix.

When the SVC is inserted in a bus, this is controlled, and thus its voltage is maintained in magnitude with a fixed value (value consigns) this makes it possible to eliminate the term $\Delta V_k = 0$(such as k is the controlled bus index). This term is substituted the difference "α" which will allows to have, after convergence, the firing angle of the thrusters which allows the maintenance of the consign voltage.

The matrix system becomes then as follows:

$$\begin{bmatrix} \Delta P_1 \\ \vdots \\ \Delta P_k \\ \vdots \\ \Delta P_n \\ \vdots \\ \Delta Q_1 \\ \vdots \\ \Delta Q_k \\ \vdots \\ \Delta Q_n \end{bmatrix} = \begin{bmatrix} \frac{\partial P_1}{\partial \delta_1} \cdots \frac{\partial P_1}{\partial \delta_k} \cdots \frac{\partial P_1}{\partial \delta_n} \frac{\partial P_1}{\partial V_1} \cdots 0 \cdots \frac{\partial P_1}{\partial V_n} \\ \vdots \\ \frac{\partial P_k}{\partial \delta_1} \cdots \frac{\partial P_k}{\partial \delta_k} \cdots \frac{\partial P_k}{\partial \delta_n} \frac{\partial P_k}{\partial V_1} \cdots 0 \cdots \frac{\partial P_k}{\partial V_n} \\ \vdots \\ \frac{\partial P_n}{\partial \delta_1} \cdots \frac{\partial P_n}{\partial \delta_k} \cdots \frac{\partial P_n}{\partial \delta_n} \frac{\partial P_n}{\partial V_1} \cdots 0 \cdots \frac{\partial P_n}{\partial V_n} \\ \frac{\partial Q_1}{\partial \delta_1} \cdots \frac{\partial Q_1}{\partial \delta_k} \cdots \frac{\partial Q_1}{\partial \delta_n} \frac{\partial Q_1}{\partial V_1} \cdots 0 \cdots \frac{\partial Q_1}{\partial V_n} \\ \vdots \\ \frac{\partial Q_k}{\partial \delta_1} \cdots \frac{\partial Q_k}{\partial \delta_k} \cdots \frac{\partial Q_k}{\partial \delta_n} \frac{\partial Q_k}{\partial V_1} \frac{\partial Q_k}{\partial \alpha} \cdots \frac{\partial Q_k}{\partial V_n} \\ \vdots \\ \frac{\partial Q_n}{\partial \delta_1} \cdots \frac{\partial Q_n}{\partial \delta_k} \cdots \frac{\partial Q_n}{\partial \delta_n} \frac{\partial Q_n}{\partial V_1} \cdots 0 \cdots \frac{\partial Q_n}{\partial V_n} \end{bmatrix} \begin{bmatrix} \Delta \delta_1 \\ \vdots \\ \Delta \delta_k \\ \vdots \\ \Delta \delta_n \\ \vdots \\ \Delta V_1 \\ \vdots \\ \Delta \alpha \\ \vdots \\ \Delta V_n \end{bmatrix} \quad (9)$$

By knowing that

$$Q_k = Q_k^{old} + Q_{svc} \quad (10)$$

Then

$$\frac{\partial Q_k}{\partial \alpha} = \frac{\partial Q_k^{old}}{\partial \alpha} + \frac{\partial Q_{svc}}{\partial \alpha} \quad (11)$$

And as Q_k depend only on the angle "α",

$$\frac{\partial Q_k}{\partial \alpha} = \frac{\partial Q_{svc}}{\partial \alpha} \quad (12)$$

$with Q_{svc} = Q_k = -V_k^2 B_{svc}$, then

$$Q_{svc} = -\frac{V_k^2}{X_C X_L}\left\{X_L - \frac{X_C}{\pi}[2(\pi - \alpha) + \sin 2\alpha]\right\} \quad (13)$$

Finally, the expression after derivation

$$\frac{\partial Q_k}{\partial \alpha} = \frac{2V_k^2}{\pi X_L}[\cos(2\alpha_{svc}) - 1] \quad (14)$$

The same case studies will be carried out as for an SVC at the beginning of line. The results obtained will be compared for the two cases of placements; and conclude if an SVC in middle of a line can ensure the compensation with the same effectiveness as two SVC placed in ends of line.

2.3 Modelling of UPFC:

The UPFC equivalent circuit shown in below Figure4 is used to derive the steady-state model. The equivalent circuit consists of two ideal voltage sources which represent the fundamental Fourier series component of the switched voltage waveforms at the AC converter terminals. The source impedances are including in the model. [4]

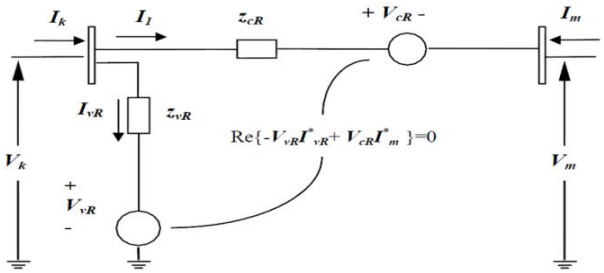

Fig 4 UPFC equivalent circuit

The UPFC voltage sources are:

$$E_{vr} = V_{vr}(\cos \delta_{vr} + j \sin \delta_{vr}) \quad (15)$$
$$E_{cr} = V_{cr}(\cos \delta_{cr} + j \sin \delta_{cr}) \quad (16)$$

Where V_{vr} and δ_{vr} are the controllable magnitude ($V_{vrmin} \leq V_{vr} \leq V_{vrmax}$) and phase angle ($0 \leq \delta_{vr} \leq 2\pi$)of the voltage source representing the shunt converter. The magnitude V_{cr} and phase angle δ_{cr} of the voltage source representing the series converter are controlled between limits ($V_{crmin} \leq V_{cr} \leq V_{crmax}$) and phase angle($0 \leq \delta_{cr} \leq 2\pi$), respectively.

Based on the equivalent circuit shown in Figure4, the active and reactive power equations are:

At bus k:

$$P_k = V_k^2 G_{kk} + V_k V_m [G_{km} \cos(\theta_k - \theta_m) + B_{km} \sin(\theta_k - \theta_m)] + V_k V_{cr} [G_{km} \cos(\theta_k - \delta_{cr}) + B_{km} \sin(\theta_k - \delta_{cr})] + V_k V_{vr} [G_{km} \cos(\theta_k - \delta_{vr}) + B_{km} \sin(\theta_k - \delta_{vr})] \quad (17)$$

$$Q_k = -V_k^2 B_{kk} + V_k V_m [G_{km} \sin(\theta_k - \theta_m) - B_{km} \cos(\theta_k - \theta_m)] + V_k V_{cr} [G_{km} \sin(\theta_k - \delta_{cr}) - B_{km} \cos(\theta_k - \delta_{cr})] + V_k V_{vr} [G_{km} \sin(\theta_k - \delta_{vr}) - B_{km} \cos(\theta_k - \delta_{vr})] \quad (18)$$

At bus m:

$$P_m = V_m^2 G_{mm} + V_m V_k [G_{mk} \cos(\theta_m - \theta_k) + B_{mk} \sin(\theta_m - \theta_k)] + V_m V_{cr} [G_{mm} \cos(\theta_m - \delta_{cr}) + B_{mm} \sin(\theta_m - \delta_{cr})] \quad (19)$$

$$Q_k = -V_m^2 B_{mm} + V_m V_k [G_{mk} \sin(\theta_m - \theta_k) - B_{mk} \cos(\theta_m - \theta_k)] + V_m V_{cr} [G_{mm} \sin(\theta_m - \delta_{cr}) - B_{mm} \cos(\theta_m - \delta_{cr})] \quad (20)$$

At series converter:

$$P_{cr} = V_{cr}^2 G_{mm} + V_{cr} V_k [G_{km} \cos(\delta_{cr} - \theta_k) + B_{km} \sin(\delta_{cr} - \theta_k)] + V_{cr} V_m [G_{mm} \cos(\delta_{cr} - \theta_m) + B_{mm} \sin(\delta_{cr} - \theta_m)] \quad (21)$$

$$Q_k = -V_{cr}^2 B_{mm} + V_{cr} V_k [G_{km} \sin(\delta_{cr} - \theta_k) - B_{km} \cos(\delta_{cr} - \theta_k)] + V_{cr} V_m [G_{mm} \sin(\delta_{cr} - \theta_m) - B_{mm} \cos(\delta_{cr} - \theta_m)] \quad (22)$$

At shunt converter:

$$P_{vr} = V_{vr}^2 G_{vr} + V_{vr} V_k [G_{vr} \cos(\delta_{vr} - \theta_k) + B_{vr} \sin(\delta_{vr} - \theta_k)] \quad (23)$$

$$Q_{vr} = -V_{vr}^2 B_{vr} + V_{vr} V_k [G_{vr} \sin(\delta_{vr} - \theta_k) - B_{vr} \cos(\delta_{vr} - \theta_k)] \quad (24)$$

UPFC Jacobian equation:

As the various network controls interact with each other, the reliability of convergence becomes the main concern in the modelling of controllable devices. Following the same line of reasoning used with all other controllable plant components models described previously, the state variables corresponding to the UPFC are combined with the network nodal voltage magnitudes and angles in a single frame-of-reference for a unified, iterative solution through a Newton-Raphson technique. The UPFC state variables are adjusted automatically so as to satisfy specified power flows and voltage magnitudes.

The UPFC linearised power equations [6] are combined with the linearised system of equations corresponding to the rest of the network,

$$[f(X)] = [J][\Delta X]$$

$$\begin{bmatrix} \Delta P_k \\ \Delta P_m \\ \Delta Q_k \\ \Delta Q_m \\ \Delta P_{mk} \\ \Delta Q_{mk} \\ \Delta P_{bb} \end{bmatrix} = \begin{bmatrix} \frac{\partial P_k}{\partial \theta_k} & \frac{\partial P_k}{\partial \theta_m} & \frac{\partial P_k}{\partial V_k} V_k & \frac{\partial P_k}{\partial V_m} V_m & \frac{\partial P_k}{\partial \delta_{cr}} & \frac{\partial P_k}{\partial V_{cr}} V_{cr} & \frac{\partial P_k}{\partial \delta_{vr}} \\ \frac{\partial P_k}{\partial \theta_k} & \frac{\partial P_m}{\partial \theta_m} & \frac{\partial P_m}{\partial V_k} V_k & \frac{\partial P_m}{\partial V_m} V_m & \frac{\partial P_m}{\partial \delta_{cr}} & \frac{\partial P_m}{\partial V_{cr}} V_{cr} & 0 \\ \frac{\partial Q_k}{\partial \theta_k} & \frac{\partial Q_k}{\partial \theta_m} & \frac{\partial Q_k}{\partial V_k} V_k & \frac{\partial Q_k}{\partial V_m} V_m & \frac{\partial Q_k}{\partial \delta_{cr}} & \frac{\partial Q_k}{\partial V_{cr}} V_{cr} & \frac{\partial P_k}{\partial \delta_{vr}} \\ \frac{\partial Q_m}{\partial \theta_k} & \frac{\partial Q_m}{\partial \theta_m} & \frac{\partial Q_m}{\partial V_k} V_k & \frac{\partial Q_m}{\partial V_m} V_m & \frac{\partial Q_m}{\partial \delta_{cr}} & \frac{\partial Q_m}{\partial V_{cr}} V_{cr} & 0 \\ \frac{\partial P_{mk}}{\partial \theta_k} & \frac{\partial P_{mk}}{\partial \theta_m} & \frac{\partial P_{mk}}{\partial V_k} V_k & \frac{\partial P_{mk}}{\partial V_m} V_m & \frac{\partial P_{mk}}{\partial \delta_{cr}} & \frac{\partial P_{mk}}{\partial V_{cr}} V_{cr} & 0 \\ \frac{\partial Q_{mk}}{\partial \theta_k} & \frac{\partial Q_{mk}}{\partial \theta_m} & \frac{\partial Q_{mk}}{\partial V_k} V_k & \frac{\partial Q_{mk}}{\partial V_m} V_m & \frac{\partial Q_{mk}}{\partial \delta_{cr}} & \frac{\partial Q_{mk}}{\partial V_{cr}} V_{cr} & 0 \\ \frac{\partial P_{bb}}{\partial \theta_k} & \frac{\partial P_{bb}}{\partial \theta_m} & \frac{\partial P_{bb}}{\partial V_k} V_k & \frac{\partial P_{bb}}{\partial V_m} V_m & \frac{\partial P_{bb}}{\partial \delta_{cr}} & \frac{\partial P_{bb}}{\partial V_{cr}} V_{cr} & \frac{\partial P_{bb}}{\partial \delta_{vr}} \end{bmatrix} \begin{bmatrix} \Delta\theta_k \\ \Delta\theta_m \\ \frac{\Delta V_k}{V_k} \\ \frac{\Delta V_m}{V_m} \\ \Delta\delta_{cr} \\ \frac{\Delta V_{cr}}{V_{cr}} \\ \Delta\delta_{vr} \end{bmatrix} \quad (25)$$

2.4 Power injection model of UPFC

A UPFC can be represented by two voltage sources representing fundamental components of output voltage waveforms of the two converter and impedance being leakage reactance's of the two coupling transformer. Voltage sources V_{se} and V_{sh} are controllable in both their magnitudes and phase angle, r and ɣ respectively the magnitude and phase angle of series respectively the magnitude and phase angle of series voltage source.

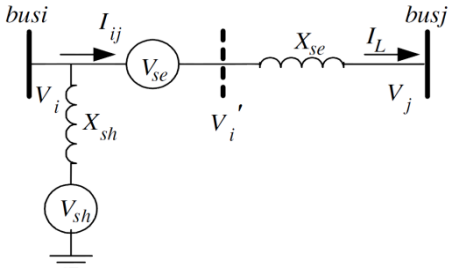

Fig 5 Two voltage-source model of UPFC

Series connected voltage source converter:

A model for UPFC which will be referred as UPFC injection model is derived. This model is helpful in understanding the impact of the UPFC on the power system in the steady state. Furthermore, UPFC injection model can easily be incorporated in the steady state power flow model.

Since the series voltage source converter does the main function of the UPFC, it is appropriate to discuss the modelling of a series voltage source converter first. Voltage of bus iis taken as reference vector, $V_i = V_i\angle 0°$and

$$V_i^{'} = V_{se} + V_i$$

The voltage source, V_{se} and is controllable in both their magnitude and phase angles

$$V_{se} = rV_i e^{-i\gamma}$$

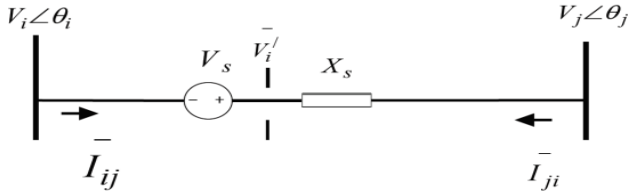

Fig 6 Representation of a Series connected VSC

The voltage source operating within the following specified limits given by

$$0 \le r \le r_{max} \text{ and} 0 \le \gamma \le 2\pi$$

The model is developed by replacing voltage source V_{se} by a current source I_{se} parallel with the transmission line as shown below figure where we know that

$$B_{se} = 1/X_{se} \quad (26)$$

$$I_{se} = -jB_{se}V_{se} \quad (27)$$

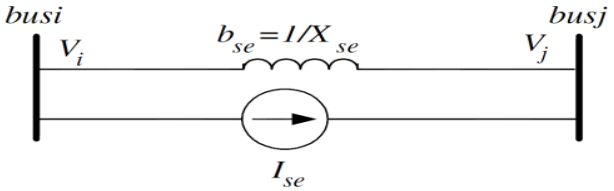

Fig 7 Replacement of series voltage source by a current source

The current source I_{se} can be modelled by injection power at two auxiliary *i*and *j*.

$$S_{is} = V_i(-I_{se})^* \quad (28)$$

$$S_{js} = V_j(-I_{se})^* \quad (29)$$

Injected power S_{is} and S_{js} can be simplifies, by substituting V_{se} and I_{se} in S_{is}

$$S_{is} = V_i(jb_{se}rV_i e^{-i\gamma})^* \quad (30)$$

By using Euler identity, $e^{i\gamma} = \cos\gamma + j\sin\gamma$

$$S_{is} = V_i(e^{-j(\gamma+90)}b_{se}rV_i^*) \quad (31)$$

$$S_{is} = V_i^2 b_{se} r[\cos(-\gamma - 90) + j\sin(-\gamma - 90)] \quad (32)$$

By using trigonometric identities the equation is reduced to

$$S_{is} = -rb_{se}V_i^2 \sin\gamma - jrb_{se}V_i^2 \cos\gamma \quad (33)$$

The decomposed real and imaginary components of S_{is}

$$S_{is} = P_{is} + jQ_{is} \text{ ,where}$$

$$P_{is} = -rB_{se}V_i^2 \sin\gamma \quad (34)$$

$$Q_{is} = -rB_{se}V_i^2 \cos\gamma \quad (35)$$

Similar modification can be applied to S_{js} then the final equation is

$$S_{js} = V_iV_jB_{se}r\sin(\theta_i - \theta_j + \gamma) + jV_iV_jB_{se}r\cos(\theta_i - \theta_j + \gamma) \quad (36)$$

The above equation is decomposed into its real and imaginary parts

$$S_{js} = P_{js} + jQ_{js}\text{, where}$$

$$P_{js} = V_iV_jB_{se}r\sin(\theta_i - \theta_j + \gamma) \quad (37)$$

$$Q_{js} = V_iV_jB_{se}r\cos(\theta_i - \theta_j + \gamma) \quad (38)$$

Based on above equations power injection model of the series-connected voltage source can be seen as two dependent power injections at auxiliary buses i and j.

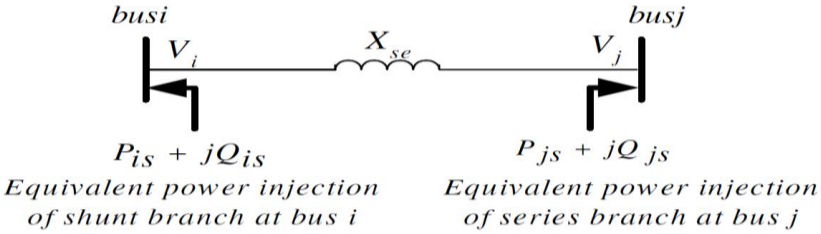

Fig 8 Equivalent power injection of series branch

Shunt converter model:

In UPFC, shunt branch is used mainly to provide both the real power, P_{series} which is injected to the system through the series branch, and the total losses within the UPFC. The total switching losses of the two converters is estimated to be about 2% of the power transferred for thyristor based PWM converter. If the losses are to be included in the real power injection of the shunt connected voltage source at bus i, P_{shunt} is equal to 1.02 times the injected series real power P_{series} through the series connected voltage source to the system.

$$P_{shunt} = -1.02P_{series}$$

The apparent power supplied by the series converter is calculated as

$$S_{series} = V_{se}I_{ij}^* = re^{-i\gamma}V_i\left(\frac{V_i^{'} - V_j}{jX_{se}}\right) \quad (39)$$

Active and reactive power supplied by the series converter can be calculated from above equation

$$S_{series} = re^{i\gamma}V_i\left(\left(re^{-i\gamma}V_i + V_i - V_j\right)/jX_{se}\right)^* \quad (40)$$

$$S_{series} = jB_{se}r^2V_i^2 + jB_{se}rV_i^2e^{j\gamma} - jB_{se}V_iV_je^{j(\theta_i - \theta_j + \gamma)} \quad (41)$$

$$S_{series} = jB_{se}r^2V_i^2 + jB_{se}rV_i^2(\cos\gamma + j\sin\gamma) - jB_{se}V_iV_j\left(\cos(\theta_i - \theta_j + \gamma) + j\sin(\theta_i - \theta_j + \gamma)\right) \quad (42)$$

From the above equation it can be decomposed into real and imaginary forms

$$S_{series} = P_{series} + jQ_{series}\text{, where}$$

$$P_{series} = rB_{se}V_iV_j\sin(\theta_i - \theta_j + \gamma) - rB_{se}V_i^2\sin\gamma \quad (43)$$

$$Q_{series} = -rB_{se}V_iV_j\cos(\theta_i - \theta_j + \gamma) + rB_{se}V_i^2\cos\gamma + r^2B_{se}V_i^2 \quad (44)$$

The reactive power delivered or absorbed by converter 1 is not considered in this model, but its effect can be modelled as a separate controllable shunt reactive source. In this case main function of reactive power is to maintain the voltage level at bus i within acceptable limits. In view of the above explanations, Q_{shunt} can be assumed to be 0. Consequently, UPFC mathematical model is constructed from the series-connected voltage source model with the addition of a power injection equivalent to $P_{shunt} + j0$ to bus i as shown below

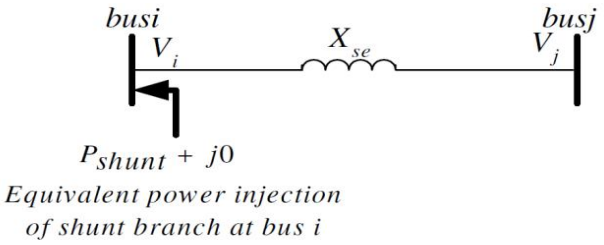

Fig 9 Equivalent power injection of shunt branch

Finally ,UPFC mathematical model can be at both bus i and j as shown below

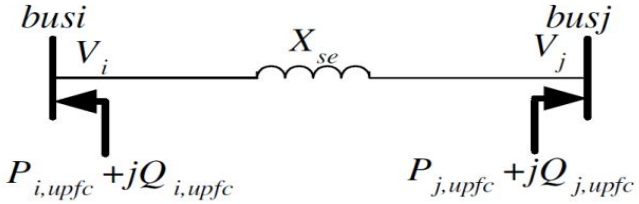

Fig 10 UPFC mathematical model

The elements of equivalent power injection in above figure is

$$P_{i,upfc} = 0.02rB_{se}V_i^2 \sin\gamma - 1.02rB_{se}V_iV_j \sin(\theta_i - \theta_j + \gamma) \quad (45)$$

$$P_{j,upfc} = rB_{se}V_iV_j \sin(\theta_i - \theta_j + \gamma) \quad (46)$$

$$Q_{i,upfc} = -rB_{se}V_i^2 \cos\gamma \quad (47)$$

$$Q_{j,upfc} = rB_{se}V_iV_j \cos(\theta_i - \theta_j + \gamma) \quad (48)$$

III. MATHEMATICAL MODEL OF OPF PROBLEM

The main goal of the OPF is to optimize a certain objective subject to several equality and inequality constraints. The problem can be mathematically modeled as follows:

$$\text{Min f (x, u)} \quad (49)$$

Objective function for cost is

$$C = a_i P_{Gi}^2 + b_i P_{Gi} + c_i$$

Where $a_i, b_i and c_i$ are cost co-efficient

subject to

$$g(x,u) \quad (50)$$

$$h_{min} \le h(x,u) \le h_{max} \quad (51)$$

where vector x denotes the state variables of a power system network that contains the slack bus real power output (P_{Gi}), voltage magnitudes and phase angles of the load buses (V_i, δ_i), and generator reactive power outputs (Q_G). Vector urepresents control variables that consist of real power generation levels (P_{GN}) and generator voltages magnitudes ($|V_{GN}|$), transformer tap setting (T_k), and reactive power injections (Q_{CK}) due to volt-amperes reactive (VAR) compensations; i.e.

$$u = [P_{G2} \dots\dots\dots P_{GN}, V_{G1} \dots\dots\dots V_{GN}, T_1 \dots\dots\dots T_{NT}, Q_{c1} \dots\dots\dots P_{cs}] \quad (52)$$

where

N = number of generator buses,

NT = number of tap changing transformers

CS = number of shunt reactive power injections.

The OPF problem has two categories of constraints:

Equality Constraints: These are the sets of non-linear power flow equations that govern the power system, i.e,

$$P_{Gi} - P_{Di} - \sum_{j=1}^{n} |V_i||V_j||Y_{ij}| \cos(\theta_{ij} - \delta_i + \delta_j) = 0 \quad (53)$$

$$Q_{Gi} - Q_{Di} - \sum_{j=1}^{n} |V_i||V_j||Y_{ij}| \sin(\theta_{ij} - \delta_i + \delta_j) = 0 \quad (54)$$

Where P_{Gi} and Q_{Gi} are the real and reactive power outputs injected at bus irrespectively, the load demand at the same bus is represented by P_{Di} and Q_{Di}, and elements of the bus admittance matrix are represented by $|Y_{ij}|$ and θ_{ij}

Inequality Constraints: These are the set of constraints that represent the system operational and security limits like the bounds on the following:

1) generators real and reactive power outputs

$$P_{Gi}^{min} \leq P_{Gi} \leq P_{Gi}^{max}, i = 1, \dots., N \quad (55)$$

$$Q_{Gi}^{min} \leq Q_{Gi} \leq Q_{Gi}^{max}, i = 1, \dots., N \quad (56)$$

2) voltage magnitudes at each bus in the network

$$V_i^{min} \leq V_i \leq V_i^{max}, i = 1, \dots, NL \quad (57)$$

3) transformer tap settings

$$T_i^{min} \leq T_i \leq T_i^{max}, i = 1, \dots, NT \quad (58)$$

4) reactive power injections due to capacitor banks

$$Q_{Ci}^{min} \leq Q_{Ci} \leq Q_{Ci}^{max}, i = 1, \dots, CS \quad (59)$$

5) transmission lines loading

$$S_i \leq S_i^{max}, i = 1, \dots., nl \quad (60)$$

IV. CO-ORDINATE CONTROL

As these devices are controlled locally so far, they do not take into account their influences on other lines or buses. Thus, a control action which is reasonable for the line or bus where the device is located might cause another line to be overloaded or voltages to take unacceptable values. Additionally, if devices are located close to each other the action of one controller can lead to a counteraction of the other controller possibly resulting in a conflicting situation. For these reasons, coordination is necessary [7], [8] and [9], especially when the number of devices increases and the distance among them decreases. Here we use Artificial Intelligence for this coordinate control. In this Artificial Intelligence Particle swam optimization is used to keep FACTS at random buses in the system and then find cost and take minimum cost.

Particle Swarm Optimization (PSO) Algorithms

Recently, Particle Swarm Optimization (PSO) algorithm [10] appeared as a promising algorithm for handling the optimization problems. PSO shares many similarities with GA optimization technique, like initialization of population of random solutions and search for the optimal by updating generations. However, unlike GA, PSO has no evolution operators such as crossover and mutation. One of the most promising advantages of PSO over GA is its algorithmic simplicity as it uses a few parameters and easy to implement. In PSO, the potential solutions, called particle, fly through the problem space by following the current optimum particles.

Here PSO technique is used for allocating the FACTS devices [10] at different location in the IEEE-30 bus system and by using OPF we obtain the cost of generation, Power loss, sum of voltage stability indices at the best location.. In this we consider two FACTS devices SVC and UPFC. Each FACTS device is places separately in the IEEE-30 bus systems.

The PSO parameters used for simulation are summarized below. Here we consider the Objective function as Cost Minimization

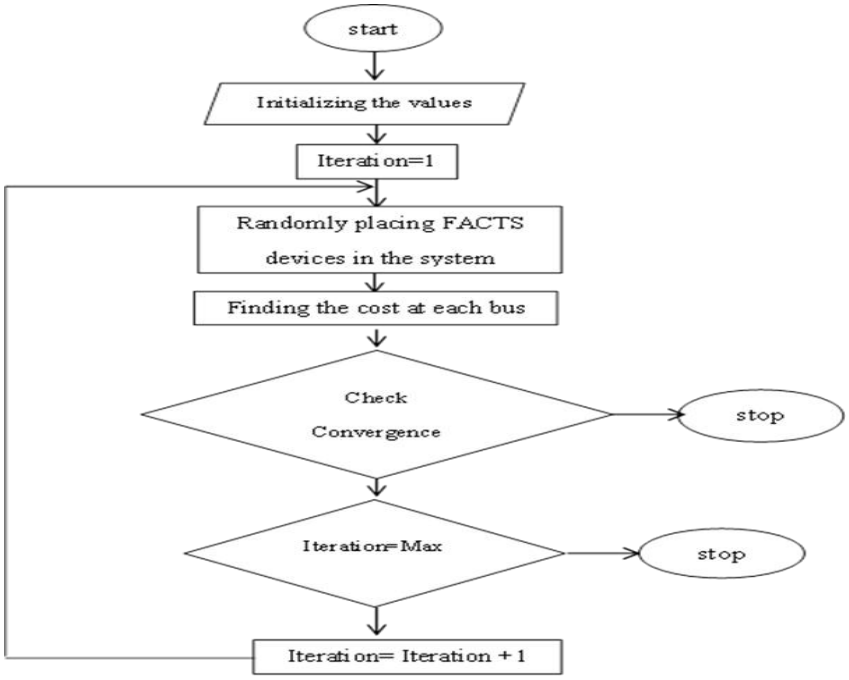

PSO Flow chart

Parameter	PSO
Population size	30
Number of iterations	150
Cognitive constant,c1:	2
Social constant,c2:	2
Inertia weight W	0.3-0.95

Optimal Parameters of PSO

IV. RESULT

The proposed PSO algorithm for solving OPF problem are tested on standard IEEE-30 bus system and the result are tabulated**.** The below Table gives the control variables, cost of generation, power loss, sum of squared voltage stability indices of the IEEE 30 bus system. Here the cost of generation is $1164.4, power loss is about 0.0810 p.u and sum squares of voltage stability indices is 0.2802 p.u for normal test bus system.

By using this PSO algorithm for solving the Optimal Power Flow problem to determine the best location and parameter setting of the SVC is applied in the IEEE 30-bus system. The best SVC locations are obtained by solving the OPF with SVC at every possible bus, and the best five locations are observed below where SVC is connected are at bus-9, bus-10, bus-12, bus-7 and bus-16. The OPF is solved with one SVC at a time by PSO technique with chosen objective function such as minimization of cost of generation. Now three SVC's connected in the system at different locations. The best location is obtained by solving the OPF with three SVC's at every possible locations, and the best locations where three SVC's are connected at bus-9, bus-10 and bus-12.

Table I Result obtained when one and many SVC's are connected in the system

Variables	Base case	Best location at one SVC is connected					three SVC's are connected buses 9,10,12
		Bus 9	Bus 10	Bus 12	Bus 7	Bus 16	
P_{G1}	1.2018	1.7788	1.7215	1.7741	1.7735	1.7823	1.7559
P_{G2}	0.9600	0.4844	0.4963	0.4921	0.4827	0.4900	0.5782
P_{G3}	0.2400	0.2071	0.2157	0.2063	0.2156	0.2183	0.2276
P_{G4}	0.2400	0.1201	0.1512	0.1192	0.1190	0.1000	0.2231
P_{G5}	0.6000	0.2136	0.2124	0.2125	0.2131	0.2140	0.4131
P_{G6}	0.2400	0.1203	0.1200	0.1200	0.1200	0.1200	0.3381
V_{G1}	1.0500	1.0886	1.0693	1.0877	1.0840	1.0869	1.0388
V_{G2}	1.0450	1.0687	1.0319	1.0687	1.0649	1.0681	0.9989
V_{G3}	1.0100	1.0400	1.0315	1.0425	1.0382	1.0408	1.0510
V_{G4}	1.0500	0.9823	1.0620	1.0831	1.0640	1.0735	1.0261
V_{G5}	1.0100	1.0362	1.0095	1.0376	1.0339	1.0364	0.9916
V_{G6}	1.0500	1.0462	1.0148	1.0715	1.0646	1.0496	1.0214
Tap-1	0.978	1.0276	1.0115	1.0142	1.0114	1.0010	0.9905
Tap-2	0.969	0.9764	1.0045	0.9662	0.9346	0.9888	1.0249
Tap-3	0.932	0.9652	1.0548	0.9727	1.0003	0.9788	1.0538
Tap-4	0.968	0.9818	0.9832	0.9746	0.9651	0.9795	0.9352
Qc_{10}	0.0	0.0207	0.0365	0.0492	0.0500	0.0438	0.0374
Qc_{12}	0.0	0.0303	0.0294	0	0.0248	0.0254	0.0164
Qc_{15}	0.0	0.0242	0.0338	0.0348	0.0500	0.0403	0.0346
Qc_{17}	0.0	0.0270	0.0114	0.0439	0.0191	0.0406	0.0265
Qc_{20}	0.0	0.0500	0.0210	0.0298	0.0316	0.0411	0.0098
Qc_{21}	0.0	0.0453	0.0325	0.0287	0.0500	0.0320	0.0309
Qc_{23}	0.0	0.0266	0.0287	0.0303	0.0389	0.0376	0.0218
Qc_{24}	0.0	0.0500	0.0432	0.0500	0.0279	0.0500	0.0175
Qc_{29}	0.0	0.0375	0.0157	0.0188	0	0.0293	0.0231
Lj2s	0.2802	0.0903	0.1516	0.1420	0.1359	0.1313	0.1738
Cost($/hr)	1164.4	800.3453	799.4987	800.3289	800.3665	800.4183	1062.2
P loss(p.u.)	0.0810	0.0903	0.0831	0.0902	0.0899	0.0907	0.1353
Cpu time(s)	-	-	-	-	-	-	370.50

The above Table I gives the control variables, cost of generation, power loss, sum of squared voltage stability indices and CPU time of the algorithm without and with SVC.It can be observed from Table that the cost of generation reduced from $1164.4 with base case to $799.4967 with one SVC and increased to

$1062.2with three SVC's. The power loss is 0.0801p.u with base case and0.0831p.u. samewith one SVCit get increased to0.1353p.u. withthree SVC's at best location. The sum of squared voltage stability indices is decreased to 0.1738 compared with base case and increased compared to with oneSVC. Also it can be observed from the Table I that the CPU time of the algorithm is 370.50.Here from the Table II the bus voltages, Equivalent susceptance and Reactive power are shown below

Table II Results of Bus voltage, Susceptance and Reactive power

	Bus 9	**Bus 10**	**Bus 12**	**Bus 7**	**Bus 16**
V_k	1.0500	1.0019	1.0500	1.0343	1.0452
B_{svc}	0.5454	0.0088	-0.1334	0.1105	0.0341
Q_{svc}	-0.601	-0.0089	0.1471	-0.1182	-0.0372
Three svc's are connected in the system					
V_k	1.0269	1.0412	1.0430	-	-
B_{svc}	-0.1349	0.6344	0.7047	-	-
Q_{svc}	0.1423	-0.6878	-0.7665	-	-

The proposed PSO algorithm for solving the optimal power flow problem to determine the optimal location and parameter setting of UPFC is applied on the IEEE 30-bus test system. The best UPFC locations are obtained by solving the OPF with UPFC in every possible line, the best five locations found are the lines connected between busses bus 9-10, bus 13- 28, bus 27- 29, bus 27- 30 and bus 8-11. The OPF is solved with one UPFC at a time by PSO technique with chosen objective function such as minimization of cost generation. Now we consider two UPFC's then the best four locations where two UPFC's are connected in the system are bus 9-10 & bus 13-28, bus 9-10 & bus 27–29, bus 9-10 & bus 27-30 and bus 9 -10 & bus 8-11 is observed in below table.

Table III Result when one and many UPFC are connected in the system

variables	**Cost objective with one UPFC**					**Cost objective with two UPFC**			
	9-10	13-28	27-29	27-30	8-11	9-10 & 13-28	9-10 & 27-29	9-10 & 27-30	9-10 & 8-11
P_{G1}	1.7750	1.7251	1.7489	1.7713	1.7635	1.7823	1.8421	1.7652	1.7640
P_{G2}	0.4871	0.5094	0.4927	0.4913	0.4845	0.4506	0.4644	0.4878	0.4832
P_{G3}	0.2091	0.1926	0.2129	0.2085	0.2246	0.1758	0.1601	0.2139	0.2244
P_{G4}	0.1204	0.1000	0.1326	0.1214	0.1187	0.1107	0.1286	0.1248	0.1180
P_{G5}	0.2138	0.2310	0.2156	0.2123	0.2141	0.1996	0.2134	0.2147	0.2166
P_{G6}	0.1200	0.1760	0.1200	0.1204	0.1200	0.1904	0.1200	0.1200	0.1200
V_{G1}	1.0853	0.9763	1.0840	1.0856	1.0847	1.0574	1.0906	1.0855	1.0911
V_{G2}	1.0666	0.9827	1.0466	1.0675	1.0656	1.0469	1.0673	1.0670	1.0718
V_{G3}	1.0403	1.0240	1.0364	1.0409	1.0359	1.0254	1.0500	1.0404	1.0439
V_{G4}	1.0417	1.0671	1.0187	1.0999	1.0676	0.9659	1.0209	1.0227	1.1000
V_{G5}	1.0370	1.0290	1.0328	1.0358	1.0326	1.0200	1.0382	1.0379	1.0425
V_{G6}	1.0555	1.0631	1.0725	1.0546	1.0706	1.0524	1.0004	1.0731	1.0508
Tap-1	1.1000	1.0346	1.0447	1.0302	0.9677	0.9709	0.9985	0.9978	1.0381
Tap-2	0.9000	0.9567	0.9009	0.9151	0.9637	0.9269	0.9876	0.9799	0.9660
Tap-3	0.9712	1.0328	1.0217	0.9799	1.0094	0.9703	1.0065	1.0037	0.9773
Tap-4	0.9605	0.9005	1.0400	0.9985	0.9520	0.9792	0.9858	1.0940	0.9680
Qc_{10}	0.0403	0.0500	0.0251	0.0208	0.0224	0.0149	0.0214	0.0297	0.0335
Qc_{12}	0.0365	0.0098	0.0292	0.0360	0.0434	0.0162	0.0204	0.0207	0.0094
Qc_{15}	0.0331	0	0.0306	0.0218	0.0128	0.0286	0.0040	0.0155	0.0200
$Qc1_7$	0.0328	0.0415	0.0142	0.0167	0.0486	0.0241	0.0341	0.0358	0.0278
Qc_{20}	0.0244	0.0380	0.0354	0.0139	0	0.0472	0.0419	0.0242	0.0175
Qc_{21}	0.0461	0.0432	0.0281	0.0392	0.0052	0.0231	0.0281	0.0027	0.0321
Qc_{23}	0.0110	0.0219	0.0155	0.0296	0.0326	0.0159	0.0241	0.0158	0.0402
Qc_{24}	0.0278	0.0240	0.0106	0.0421	0.0276	0.0465	0.0354	0.0029	0.0044
Qc_{29}	0.0251	0.0323	0	0.0330	0.0209	0.0291	0.0327	0.0118	0.0341
Cost ($/h)	800.8074	806.3261	799.1642	800.7728	801.1624	797.047	801.020	801.410	801.5196
P loss(p.u.)	0.0914	0.1000	0.0924	0.0912	0.0913	0.0755	0.0947	0.0923	0.0923
Lj^2 sum	0.1744	0.1684	0.1338	0.1478	0.1508	0.1622	0.3540	0.2559	0.1565
t	283.9530	416.8750	278.3590	250.7500	246.3910	497.781	421.344	360.093	447.6410

The above Table III gives the control variables, cost of generation, power loss, sum of squared voltage stability indices, and CPU time of the algorithm without and with UPFC.The best location are at bus 27-29 when one UPFC is connected and bus 9-10 and bus 13-28 when two UPFC's are connected in IEEE-30 bus system. It can be observed from Table that the cost of generation reduced from $1164.4 with base case to $799.164 with one UPFC and reduce to $797.0479 with two UPFC's. The power loss is increased from 0.0801 p.u with base case to 0.0924 p.u. with one UPFC and reduce to 0.0755 p.u. with two UPFC's at best location.

The sum of squared voltage stability indices is decreased to 0.1622 compared with base case and one UPFC. Also it can be observed from the Table that the CPU time of the algorithm is 497.7810 more compared with one UPFC.

V. CONCLUSION

FACTS Devices have many benefits by using in the transmission line. But an uncoordinated utilization of such devices may results in conflicting situation which can endanger the operation of transmission. Thus, a Co-ordinate control based on Optimal Power Flow has been developed in this paper. The Objective function was analyzed in simulation with different combination of FACTS devices. It was demonstrated that each devices is able to influence certain parts of objective function. SVC's are responsible for the part dealing with voltage and active power losses and UPFC is used for Reactive power flow in the IEEE-30 bus system. Finally simulation show improvement of derived control was presented: voltage profile has become more balanced and active power losses were reduced.

REFERENCES

[1]. H. Ambriz-Perez, E. Acha, and C. R. Fuerte-Esquivel, "Advanced SVC models for Newton-Raphson load flow and Newton optimal power flow studies," Power Systems, IEEE Transactions on, vol. 15, pp. 129-136, 2000.

[2]. N. G. Hingorani and L. Gyugyi, Understanding FACTS concepts and technology of flexible AC transmission systems. New York: IEEE Press, 2000.

[3]. N. Aouzellag LAHAÇANI, B. MENDIL, "Modelling and Simulation of the SVC for Power System Flow Studies: Electrical Network in voltage drop" , Leonardo Journal of Sciences,issue 13, pp. 153-170, July-December 2008

[4]. G. T. Heydt , Douglas J. Gotham: "Power flow control and power flow studies for systems FACTS devices", IEEE Transactions on Power Systems, Vol. 13, No. 1, February 1998.

[5]. L. Gyugyi, C. D. Schauder, S. L. Williams, T. R. Rietman, D. R. Torgerson, and A. Edris, "The unified power flow controller: A new approach to power transmission control," IEEE Trans. Power Del., vol. 10, no. 2, pp. 1085–1097, Apr. 1995.

[6]. Enrique Acha, Claudio R. Fuerte-Esquivel Hugo Ambriz-Perez, Cesar Angeles-CamaCho "Modelling and simulation in power networks" by John Wiley & Sons.

[7]. A. Oudalov, "Coordinated control of multiple FACTS devices in an electric power system." Diss. EPF Lausanne, 2003, pp. 190.

[8]. Siddhartha Panda and Narayana Prasad Padhy, "Coordinated Design of TCSC Controllers and PSSS Employing Particle Swarm Optimization Technique," International Journal of Computer and Information Science and Engineering, Vol.1, No.1, 2006.

[9]. S. Panda, N. P. Pandy, and R. N. Patel, "Robust Coordinated Design of PSS and TCSC Using PSO Technique for Power System Stability Enhancement," Journal of Electrical Systems, 3-2(2007), pp.109-123.

[10]. Amrane,Y.;Boudour,M ; Ladjici,A "Particle swarm optimization based reactive power planning for line stability improvement" IEEE conference publication ,pp 1-6 ,2015.

[11]. Ahsan,M.A; Eakul Islam, S.M ; Ghosh,B.C. "Performance analysis of different searching algorithm in optimization of power system operation in optimization of power system operation" IEEE conference publication ,pp 1-6,2014

[12]. BindeshwarSingh,N.k. Sharma and A.N. Tiwari , "A Comprehensive Survey of Optimal Placement and Coordinated Control Techniques of FACTS Controllers in Multi-Machine Power System Environments" Journal of electrical eng and tech,vol 5,pp 79-102,2010.